

Direct Observation of Photocontrolled Ion Release: A Nanosecond Time-Resolved Spectroscopic Study of a Benzothiazolium Styryl Azacrown Ether Dye Complexed with Barium

Igor K. Lednev,[†] Ronald E. Hester, and John N. Moore*

Department of Chemistry, The University of York, Heslington, York YO1 5DD, U.K.

Received: July 18, 1997[⊗]

A benzothiazolium styryl azacrown ether dye (**1**) and its photocontrolled complexation with Ba²⁺ in acetonitrile solution have been studied by nanosecond time-resolved UV–visible absorption spectroscopy. Continuous visible irradiation of *trans*-**1** in the presence of Ba²⁺ was used to generate a photostationary-state mixture with “closed” *cis*-**1**–Ba²⁺ present in high concentration: in this form, the barium cation is complexed with both the azacrown and a propylsulfonate group pendant to the benzothiazolium dye. A nanosecond UV photolysis pulse was used to induce photoisomerization of this “closed” *cis*-**1**–Ba²⁺ species. Time-resolved UV–visible absorption studies have revealed that the barium cation initially remains complexed to the azacrown in the *trans*-isomer formed <50 ns after UV photolysis and that the cation is subsequently released from the azacrown on a time scale of ca. 700 ns, consistent with the equilibrium composition of the solution expected from the thermal chemistry under these conditions. Along with time-resolved and steady-state studies of the effect of temperature and cation concentration, these studies have enabled a quantitative mechanism to be proposed for the thermal and photochemical ion-complexing properties of this dye. These direct observations demonstrate that sustained, photocontrolled ion release from an azacrown ether dye can be achieved within 1 μs of photolysis.

Introduction

The design and study of molecular devices capable of photocontrolled release or complexation of cations in solution is currently an active area of interdisciplinary research.^{1,2} There is a substantial effort in the design and synthesis of new molecules and supramolecular systems, in studies of their thermal chemistry and photochemistry, and in exploring their use within molecular devices and sensors, with potential applications ranging from molecular electronics to biomedicine. Typically, the molecules designed for photocontrolled ion complexation comprise a chromophore linked to a macrocyclic ionophore, with photoexcitation of the chromophore inducing a structural change which modifies the stability constant for ion complexation at the macrocycle and leads to ion capture or ion release.³ In addition to the design and testing of such molecules for their efficiency in particular reactions, it is important to develop a quantitative understanding of the reaction mechanisms and their dependence on molecular structure. A detailed understanding of the way in which structure influences the underlying thermodynamics and kinetics which delineate the thermal and photochemical reaction pathways may be used to inform strategies for improved molecular design.

There has been substantial progress in the study of mechanisms in the thermal reactions of macrocyclic ionophores for ion capture and ion release,^{4–6} with NMR, ultrasonic absorption, and stopped-flow techniques being used to study the kinetics of these reactions. Many molecular systems have been developed for photocontrolled ion release,^{3,7–10} and the use of light as the trigger for reaction now provides the opportunity to study the kinetics and reaction mechanisms of ion capture and ion release by pulsed laser excitation and time-resolved spectroscopy. These techniques supplement those available for the study of thermal complexation reactions and enable excited states and

intermediates to be monitored directly on time scales as short as 10^{–13} s. Several picosecond time-resolved spectroscopic studies of metal-complexed chromoionophores have already been reported,^{11–16} and in these cases the photochemistry was found to involve transient cation release in the excited state, with recombination occurring rapidly on electronic relaxation, within ca. 10^{–9} s, because of the structures of the specific molecules studied. These picosecond studies have provided useful information on the excited-state complexation properties of such dyes, but it is desirable to extend the application of time-resolved techniques to molecules in which cation release is sustained over a longer time scale in order to improve our understanding of mechanisms in molecular systems which may find wider application. In particular, it is important to study the time scale of photocontrolled ion release in such systems and to understand the mechanism of ion release and its dependence on molecular design; in some applications, such as studies of biochemical reactions requiring fast ion concentration jumps,^{14,17} the time scale may be as important as the yield of ion release.

Our recent studies of the thermal and photochemical ion-complexing properties of several styryl crown ether dyes^{18–22} have indicated that molecules in which an azacrown ether is linked to a benzothiazolium dye offer good opportunities for photocontrolled ion complexation and ion release and also for photocontrolled ion sensing. In particular, we have studied dye **1** (Figure 1) in detail using steady-state UV–visible absorption and emission spectroscopy and their time-resolved analogues on picosecond and kilosecond time scales.

trans-**1** is sensitive to alkaline and alkaline-earth metal cations in acetonitrile: ion selectivity is evident from the differing magnitudes of the stability constant for complexation of different cations with the azacrown and from the differing UV–visible absorption spectra of the ion-complexed forms which result in strong, ion-dependent color changes.²² Photolysis of *trans*-**1** generates an excited singlet state, with a lifetime of ca. 205 ps, which we have observed directly by time-resolved UV–visible

[†] Current address: Chevron Science Center, Department of Chemistry, Box 39, University of Pittsburgh, Pittsburgh, PA 15260.

[⊗] Abstract published in *Advance ACS Abstracts*, September 1, 1997.

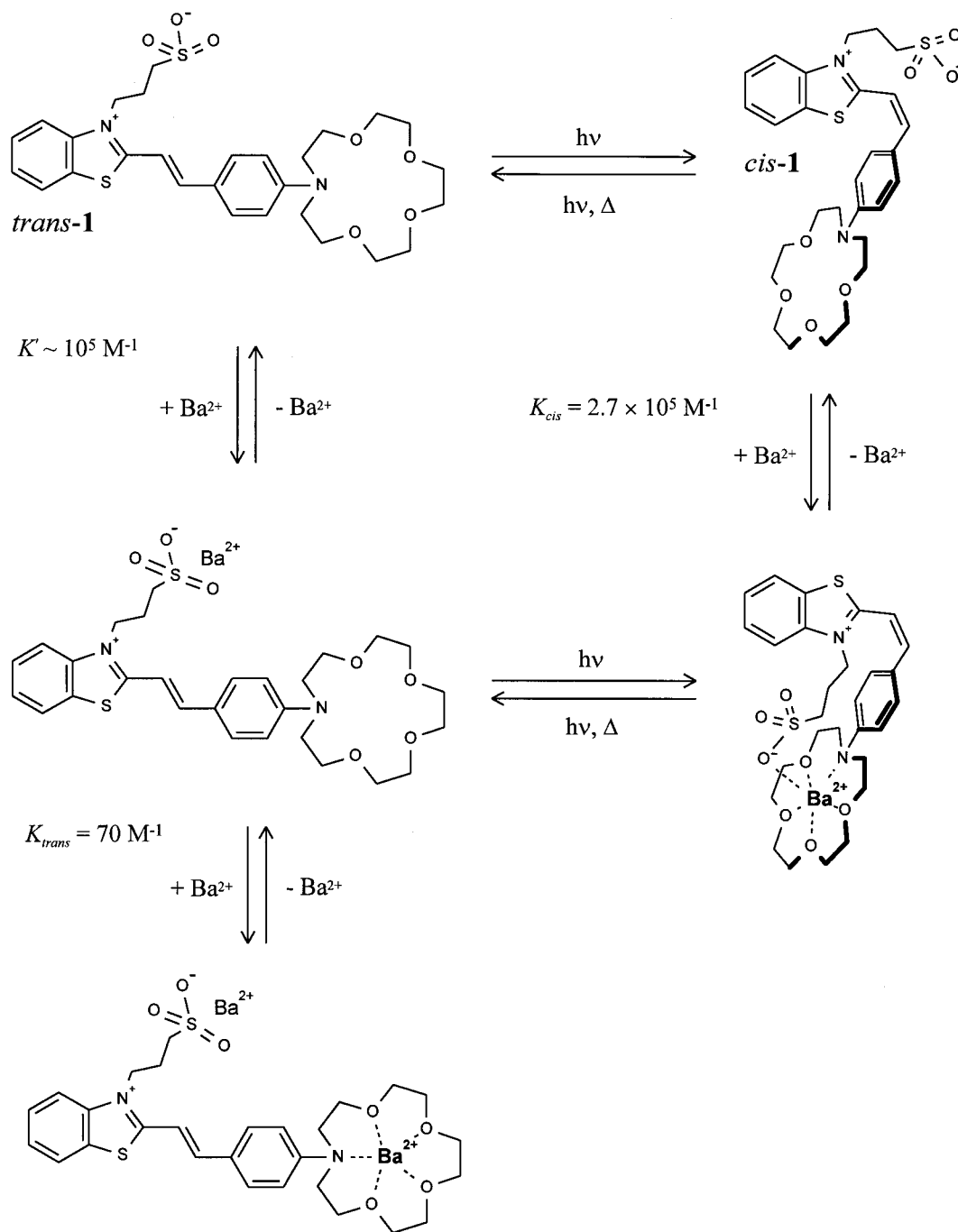


Figure 1. Mechanism for the thermal and photochemical reactions of **1** in the presence of Ba^{2+} .¹⁹

spectroscopy,²⁰ and this excited state decays by radiative and nonradiative mechanisms, including *cis*–*trans* photoisomerization as a significant route. The *cis*-isomer generated on photolysis is thermally unstable and decays in ca. 26 s to regenerate *trans*-**1**.¹⁹ Compound **1** is particularly sensitive to the presence of barium cations in acetonitrile. First, barium associates with the sulfonate group of *trans*-**1** at very low concentrations in acetonitrile, with a stability constant of $K' \approx 10^5 \text{ M}^{-1}$. Second, barium has a much higher stability constant for complexation with the azacrown of *cis*-**1** ($K_{cis} = 2.7 \times 10^5 \text{ M}^{-1}$) than for complexation with the azacrown of *trans*-**1** ($K_{trans} = 70 \text{ M}^{-1}$). The Ba^{2+} -complexed form of *cis*-**1** has a lifetime of up to 10^4 s, dependent on the Ba^{2+} concentration, and thus is much more stable to thermal isomerization than the noncomplexed form. This increased stability has been assigned to the formation of a "closed" form, *cis*-**1**– Ba^{2+} , in which the azacrown-encapsulated cation also interacts intramolecularly

with the sulfonate group (Figure 1), this additional intramolecular interaction being possible only for the *cis*-isomer because of steric constraints. The high stability constant of "closed" *cis*-**1**– Ba^{2+} has been ascribed to $\text{Ba}^{2+}/\text{SO}_3^-$ association facilitating the capture of the barium by the azacrown. Similar studies of a derivative of **1** in which the propylsulfonate group is replaced by an ethyl group²⁰ have substantiated this interpretation, which is summarized in Figure 1. Thus, we have already obtained much quantitative information on the thermal and photochemical reactions of **1**, and this has enabled us now to address the key question of the time scale and mechanism by which photocontrolled ion release can be achieved with this molecular system.

Here we report studies aimed at understanding the kinetic and mechanistic details of the reaction by which the "closed" form of *cis*-**1**– Ba^{2+} in acetonitrile regenerates *trans*-**1** on photolysis. Our strategy has been to form *cis*-**1**– Ba^{2+} at high

concentration by continuous visible irradiation of a solution of *trans*-**1** and Ba²⁺ in situ and then to photolyze this "closed" *cis*-**1**-Ba²⁺ species with a nanosecond UV pulse and use time-resolved UV-visible absorption spectroscopy to observe the subsequent reactions. We have monitored this reaction as a function of barium ion concentration and as a function of temperature. Along with steady-state studies of the dependence of the stability constant for complexation of Ba²⁺ with the azacrown of *trans*-**1** on temperature, these nanosecond time-resolved studies have enabled kinetic and thermodynamic details of the decomplexation mechanism to be obtained.

In addition to providing information on this specific molecule, these studies by direct spectroscopic observation provide important new information on more general aspects of photocontrolled ion release. The results demonstrate that sustained ion release can be achieved within ca. 1 μ s of photolysis of an azacrown ether dye. The key molecular feature that provides photocontrol is the structural change of isomerization, which occurs rapidly (within $\ll 1$ μ s). The thermal chemistry of the resulting photoisomer then drives and sustains the ion release from the azacrown after isomerization has occurred.

Experimental Section

For the nanosecond time-resolved spectroscopic studies, the sample solution comprised *trans*-**1** (ca. 2×10^{-5} M) in the presence of Ba(ClO₄)₂ (at various concentrations) in acetonitrile. This sample was contained in the inner portion (50 mm pathlength \times 10 mm diameter) of a jacketed, cylindrical quartz cell with water circulating through the outer jacket to control the sample temperature (± 1 °C). A 250 W Xe arc lamp with a 450 nm long-pass filter was used to irradiate this sample solution continuously from above, along the whole 50 mm pathlength, in order to maintain a photostationary-state mixture in which the "closed" *cis*-**1**-Ba²⁺ complex was present at high concentration. A XeCl excimer laser (Lambda Physik EMG50) provided a UV photolysis pulse (308 nm, 30 ns), with an energy of ca. 8 mJ at the sample, which was directed lengthwise through the portion of the cell containing the sample solution. A 200 W Xe arc lamp provided a pulsed (ca. 400 μ s) monitor beam which was collimated to ca. 5 mm diameter and counterpropagated lengthwise through the sample solution. Dichroic beam-splitters which transmitted the visible probe beam and reflected the UV photolysis beam were used to achieve this collinear, counterpropagating geometry. The probe beam was directed to a 0.25 m monochromator which was used at ca. 2 nm resolution. A photomultiplier tube and a 500 MHz digital storage oscilloscope (Tektronix TDS520) were used to record kinetic traces of the transmitted probe beam intensity. The data were converted to the time-dependent change in absorbance on photolysis, ΔA_t , according to $\Delta A_t = \log_{10}(I_0/I_t)$, where I_0 and I_t are the transmitted intensities before and at time t after photolysis, respectively. Typically, kinetic traces were averaged over ≤ 4 laser pulses, with an interval between pulses which was sufficient to ensure that the photostationary state was re-established. Typically, traces were collected over 5 μ s at 2 ns per data point; the 2500-point data sets were averaged over 20 points for the figures presented here. UV-visible spectra taken before and after the experiments confirmed the integrity of the sample. Control experiments were performed on a sample of *trans*-**1** and Ba(ClO₄)₂ in the absence of continuous irradiation; a sample of *trans*-**1** in the absence of both Ba(ClO₄)₂ and continuous irradiation; and a sample of *trans*-**1** in the absence of Ba(ClO₄)₂ but in the presence of continuous irradiation.

Steady-state UV-visible absorption spectra were measured with a Hitachi U-3000 spectrophotometer, and the sample was

contained in the same temperature-controlled cell, of 50 mm pathlength, used for the time-resolved experiments. The spectrum of *trans*-**1** in the presence of Ba(ClO₄)₂ (at two different concentrations) was measured first without external irradiation. In order to measure the spectrum of the photostationary state formed on continuous irradiation, the same solution was photolyzed in situ for ca. 1 min using the same lamp and geometry used for the nanosecond time-resolved experiments; the spectrometer lid was then closed, and the spectrum of the photostationary-state mixture recorded rapidly.

The SPSS software package (Statistical Package for the Social Sciences, SPSS Inc.) was used for data analysis. Fitted values are quoted with uncertainties of $\pm 2\sigma$.

The synthesis of *trans*-**1** has been described.^{21,23} Ba(ClO₄)₂ and acetonitrile (anhydrous, Aldrich) were used as received.

Results and Analysis

Nanosecond Time-Resolved Spectroscopy. Initial experiments were carried out to determine the dependence of the transient kinetics on the sample conditions. In the absence of continuous irradiation to generate a photostationary-state mixture, a solution of *trans*-**1** and Ba(ClO₄)₂ gave a rapid change in absorbance within < 50 ns (the instrument resolution), and no further changes were observed on the nanosecond-microsecond time scale studied here. Similar kinetics were obtained on photolysis of **1** in the absence of Ba(ClO₄)₂, in both the presence and absence of continuous visible irradiation. Only samples of **1** in the presence of both Ba(ClO₄)₂ and continuous irradiation resulted in a transient signal which showed changes on the nanosecond-microsecond time scale.

From our previous studies,¹⁹ we have established that continuous irradiation ($\lambda > 450$ nm) of an acetonitrile solution of *trans*-**1** and Ba(ClO₄)₂ at 10^{-4} - 10^{-3} M results in a photostationary-state mixture in which the "closed" form of *cis*-**1**-Ba²⁺ is present at high concentration. For the particular conditions used in these experiments, the sample solution prior to pulsed photolysis is estimated to comprise principally "closed" *cis*-**1**-Ba²⁺ ($\geq 70\%$) and *trans*-**1** ($\leq 30\%$) in which Ba²⁺ is associated at the propylsulfonate but is not complexed with the azacrown. The relative concentrations of 70:30 were estimated from the UV-visible absorption spectrum of the photostationary-state mixture and by assuming that the absorption at 520 nm arises only from *trans*-**1** and not from "closed" *cis*-**1**-Ba²⁺; if "closed" *cis*-**1**-Ba²⁺ does contribute to the absorption at 520 nm, then it comprises $> 70\%$ of the mixture. The UV-visible absorption spectra of photostationary-state mixtures that we have measured previously¹⁹ have enabled us to conclude that *cis*-**1**, in both Ba²⁺-complexed and cation-free forms, absorbs more strongly at 280-320 nm and more weakly at > 450 nm than *trans*-**1** in any form. In particular, the UV-visible absorption spectrum of "closed" *cis*-**1**-Ba²⁺ has a distinct band at ca. 290 nm,¹⁹ and pulsed UV photolysis within this band was used to initiate the photochemistry because the "closed" *cis*-**1**-Ba²⁺ isomer has a larger absorption coefficient in this region than the *trans*-**1** isomer, which also is present as a minor component of the sample solution.

The transient absorption kinetics following 308 nm photolysis were measured at 5-20 nm intervals throughout the range 360-600 nm, as illustrated in Figure 2 probe wavelengths of 435 and 520 nm. The transient signal comprised a rapid component (< 50 ns), corresponding to the instrument response function, and a second component which decayed on the microsecond time scale. The kinetics were analyzed at delay times after the decay of the initial component was complete (as illustrated by the range of the residuals in Figure 2) and were found to fit

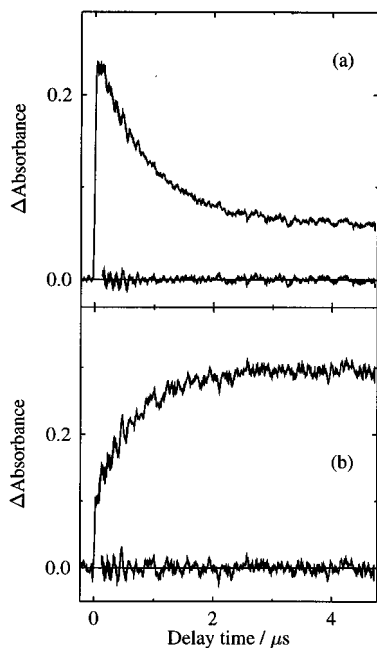


Figure 2. Nanosecond transient absorption kinetics obtained on 308 nm photolysis of a solution of **1** (ca. 2×10^{-5} M) in acetonitrile, at 21 °C, in the presence of $\text{Ba}(\text{ClO}_4)_2$ (1.9×10^{-4} M) and irradiated continuously at >450 nm. Data obtained at probe wavelengths of (a) 435 and (b) 520 nm. The residuals from the fits to eq 1 also are shown around the baseline.

well to a single-exponential decay, as given by eq 1, where ΔA_0 and ΔA_∞ are the changes in absorbance immediately and at long times after photolysis, respectively, and k_{obs} is the observed first-order rate constant:

$$\Delta A_t = \Delta A_\infty + (\Delta A_0 - \Delta A_\infty) \exp(-k_{\text{obs}} t) \quad (1)$$

The observed first-order rate constant was found to be $k_{\text{obs}} = (1.3 \pm 0.2) \times 10^6 \text{ s}^{-1}$ for a solution comprising **1** (ca. 2×10^{-5} M) and $\text{Ba}(\text{ClO}_4)_2$ (1.9×10^{-4} M), and, within experimental error, k_{obs} was found to be independent of the probe wavelength.

The time-resolved absorption spectra shown in Figure 3 (upper plot) were constructed by selecting a set of delay times and plotting ΔA_t , extracted from the fits of the kinetic data, as a function of probe wavelength.

The transient absorption kinetics were studied as a function of barium ion concentration at a fixed temperature (21 °C) over the range 1.3×10^{-4} to 1.2 M, and as a function of temperature at a fixed Ba^{2+} concentration (1.9×10^{-4} M) over the range 15–40 °C; the rate constants obtained from fitting these data are analyzed below (and presented below in Figures 6 and 7, respectively). Probe wavelengths of 434 and 520 nm were chosen for these studies because they correspond to peaks in the transient spectra (Figure 3).

Steady-State Spectroscopy. To enable the nanosecond time-resolved difference spectra to be compared with those obtained on steady-state photolysis of **1** in the presence of Ba^{2+} , two experiments were carried out using continuous irradiation at >450 nm to generate a photostationary-state mixture of two samples, which were then studied with a spectrophotometer. In one case, the spectrum **1** (3×10^{-6} M) in the presence of Ba^{2+} at high concentration (0.97 M) was obtained in the presence and absence of continuous irradiation; the data are presented as a difference spectrum (nonphotolyzed–photolyzed) in Figure 3g. This experiment was then repeated with **1** (3×10^{-6} M)

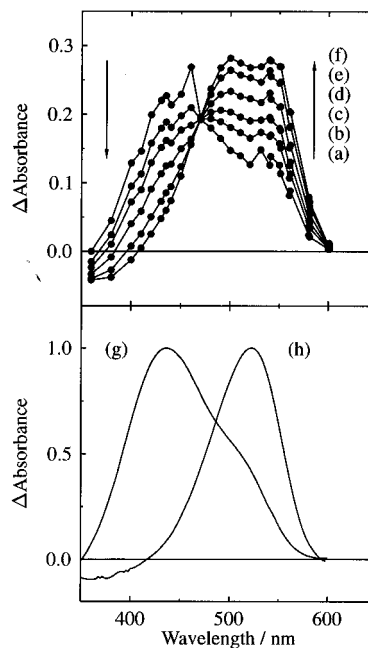


Figure 3. Upper plot: nanosecond transient absorption spectra obtained on 308 nm photolysis of a solution of **1** (ca. 2×10^{-5} M) in acetonitrile, at 21 °C, in the presence of $\text{Ba}(\text{ClO}_4)_2$ (1.9×10^{-4} M) and irradiated continuously at >450 nm. Data obtained at delay times of (a) 0.11, (b) 0.34, (c) 0.54, (d) 0.94, (e) 1.74, and (f) 4.72 μs . Data points are shown as dots, joined by solid lines. Lower plot: UV–visible difference spectra (nonphotolyzed–photolyzed) obtained on continuous photolysis at >450 nm of **1** (ca. 3×10^{-6} M) in acetonitrile, in the presence of $\text{Ba}(\text{ClO}_4)_2$ at concentrations of (g) 0.97 and (h) 2×10^{-4} M.

in the presence of Ba^{2+} at low concentration (2×10^{-4} M); the data are presented similarly as a difference spectrum in Figure 3h.

To study the temperature dependence of the stability constant for complexation of Ba^{2+} with the azacrown of *trans*-**1**, the spectra of *trans*-**1** in acetonitrile (ca. 3×10^{-6} M) were measured over the range of 15–77 °C in the presence of $\text{Ba}(\text{ClO}_4)_2$ at three different concentrations (0, 2.9×10^{-2} , and 0.97 M), as illustrated in Figure 4.

Discussion

In the absence of $\text{Ba}(\text{ClO}_4)_2$, the sample consists of *trans*-**1**, and pulsed UV photolysis results in a rapid change in absorbance, which is consistent with *trans*–*cis* photoisomerization on the picosecond time scale.²⁰ The absence of any further changes in absorbance on the nanosecond–microsecond time scale indicates that the combined intensity of the continuous lamp (generating the photostationary state) and the pulsed lamp (providing the monitor beam) does not result in significant photoalteration of the sample on this time scale. A similar result in the presence of $\text{Ba}(\text{ClO}_4)_2$ but the absence of continuous irradiation arises similarly because the photoisomerization process occurs on the picosecond time scale and the lamp irradiation causes no photoalteration on the time scale of observation. Thermal *cis*–*trans* isomerization occurs on a time scale of ≥ 20 s.¹⁹

In the absence of continuous irradiation, the sample solution consists of *trans*-**1** in the noncomplexed form ($\leq 4.5\%$), in the $\text{Ba}^{2+}/\text{SO}_3^-$ associated form ($\geq 95\%$), and in the form (1.5%) in which one Ba^{2+} is associated with the SO_3^- group and another Ba^{2+} is complexed with the azacrown, as estimated from the equilibrium constants determined by earlier work (Figure 1).¹⁹ Under continuous irradiation with visible light ($\lambda > 450$ nm),

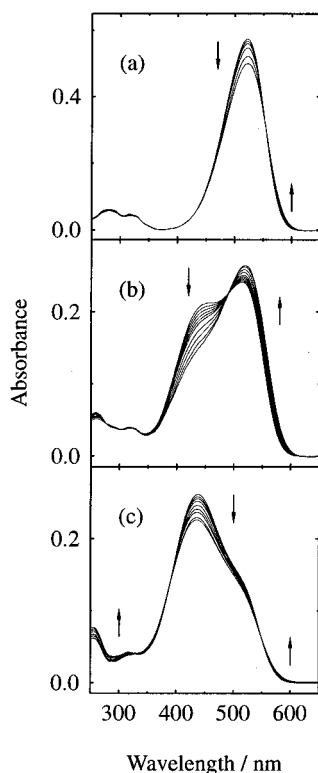


Figure 4. UV-visible absorption spectra of *trans*-**1** in acetonitrile (ca. 3×10^{-6} M), measured as a function of temperature over the range 15–77 °C: (a) in the absence of $\text{Ba}(\text{ClO}_4)_2$ and in the presence of $\text{Ba}(\text{ClO}_4)_2$ at (b) 2.9×10^{-2} and (c) 0.97 M. Arrows indicate the direction of change on increasing the temperature.

we have established that a photostationary state is formed, within ca. 30 s, in which “closed” *cis*-**1**- Ba^{2+} ($\geq 70\%$) is the dominant form. “Closed” *cis*-**1**- Ba^{2+} absorbs more strongly at 308 nm than *trans*-**1**, and this results in the UV photolysis pulse being absorbed predominantly ($\geq 85\%$) by “closed” *cis*-**1**- Ba^{2+} . The control experiments have established that the small contribution from *trans*-**1** will give only an offset, produced within the instrument response function, and no changes in absorbance on the nanosecond–microsecond time scale of observation; only the photochemistry of “closed” *cis*-**1**- Ba^{2+} will contribute to the time-dependent changes on this time scale. Thus, the reactant for these time-resolved experiments is best described as “closed” *cis*-**1**- Ba^{2+} .

UV photolysis of “closed” *cis*-**1**- Ba^{2+} may be expected to result in *cis*-*trans* photoisomerization first to form *trans*-**1**- Ba^{2+} , and the initial changes that occur in < 50 ns are consistent with the time scale that may be expected for photoisomerization of this species.²⁰ The dual intramolecular interaction of the Ba^{2+} cation with both sulfonate and azacrown groups is possible only for the *cis*-isomer, because of steric constraints, and so one interaction must be lost during the *cis*-*trans* isomerization reaction which is induced by UV photolysis. Thus, the initial form of the *trans*-**1**- Ba^{2+} complex is likely to have one of two possible structures: the barium is likely either to be associated with the sulfonate group or to be encapsulated within the azacrown ether, as shown schematically in Figure 5. If the barium remains associated initially with the sulfonate group, then no further changes in the absorption spectrum would be expected to occur for ca. 10 s: the $\text{Ba}^{2+}/\text{SO}_3^-$ associated form is dominant at thermal equilibrium (as discussed above) and the low intensity of the continuous irradiation beam reestablishes the photostationary-state mixture by regenerating the “closed” *cis*-**1**- Ba^{2+} form on this longer time scale. If the barium remains bound initially to the azacrown group, then it

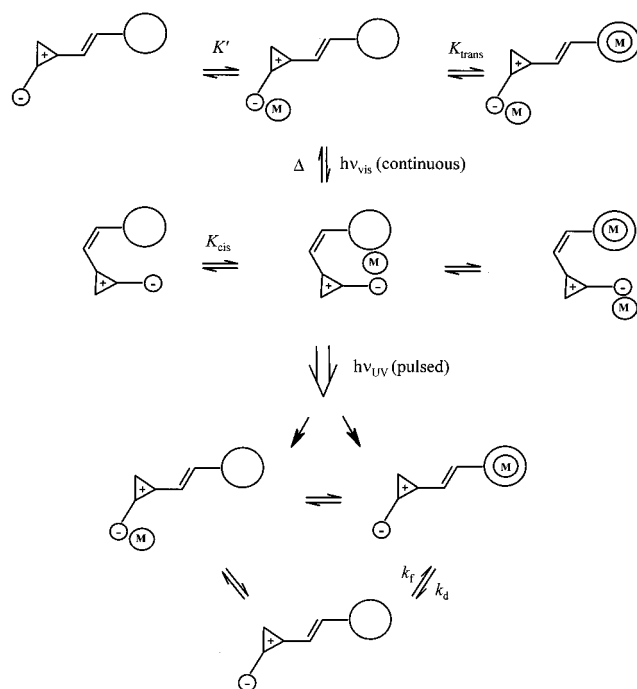


Figure 5. Schematic mechanism for the thermal and photochemical reactions of **1** in the presence of Ba^{2+} , with continuous visible and pulsed UV irradiation.

would be expected subsequently to dissociate thermally, ultimately to form the more stable $\text{Ba}^{2+}/\text{SO}_3^-$ associated form, which is dominant at thermal equilibrium. Steady-state studies have established that the UV-visible spectrum of *trans*-**1** is insensitive to $\text{Ba}^{2+}/\text{SO}_3^-$ association, but that it changes significantly on Ba^{2+} /azacrown complexation and on *trans*-*cis* photoisomerization.¹⁹ Thus, if barium remains associated initially with the sulfonate, then a large change in the absorption spectrum would be expected within 1 ns of photolysis, due to isomerization and dissociation from the azacrown, with no further changes for ca. 10 s; alternatively, if barium remains bound initially to the azacrown, then a large change would be expected within 1 ns, due to isomerization, followed by another large change between 1 ns and 1 ms^{4–6} as the cation is released. The time-resolved data, which show two large changes in the UV-visible absorption spectrum on time scales of < 50 ns and ca. 700 ns, indicate that the latter mechanism operates.

This interpretation is substantiated further by the profiles of the time-resolved spectra. The steady-state difference spectrum (nonphotolyzed–photolyzed) obtained on photolysis of **1** in the presence of Ba^{2+} at 0.97 M (Figure 3g) shows the change in absorbance on going from a photostationary-state mixture in which *cis*-**1**- Ba^{2+} is dominant to *trans*-**1**, in which one barium is associated with the sulfonate and a second barium is encapsulated by the azacrown. The steady-state difference spectrum obtained at a lower Ba^{2+} concentration of 2×10^{-4} M (Figure 3h) shows the change on going from a photostationary-state mixture in which “closed” *cis*-**1**- Ba^{2+} is dominant to *trans*-**1**, in which barium is associated only with the sulfonate group and not with the azacrown. A comparison of these steady-state difference spectra with the nanosecond time-resolved difference spectra shows clearly that the spectrum at early times after photolysis (Figure 3a; 110 ns) resembles that in going from “closed” *cis*-**1**- Ba^{2+} to *trans*-**1** with barium encapsulated in the azacrown, whereas that at long times after photolysis (Figure 3f; 4.7 μs) resembles that in going from “closed” *cis*-**1**- Ba^{2+} to *trans*-**1** with barium released from the azacrown.

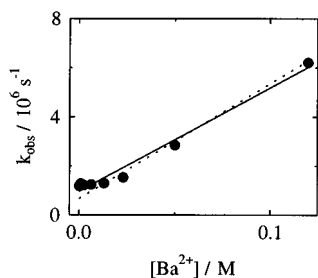
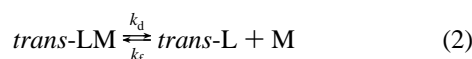


Figure 6. Dependence of k_{obs} on $[\text{Ba}^{2+}]$, measured at 21 °C, fitted to eq 3 with no constraint on the fitted values (solid line) and fitted to eq 4 with K_{trans} fixed at 70 M^{-1} (dotted line).

Taken together, the transient kinetics and spectra indicate that the photochemical mechanism involves initial *cis*–*trans* photoisomerization in <50 ns, with the barium retained within the azacrown, and subsequent release of the barium from the azacrown in ca. 700 ns. The release mechanism is given by reaction 2, where L is the azacrown ligand, M is the metal cation, and k_{d} and k_{f} are the rate constants for dissociation and formation of the complex, respectively:



For conditions in which the initial concentration of the azacrown– Ba^{2+} complex is greater than its equilibrium concentration, i.e. $[\text{trans-LM}]_0 > [\text{trans-LM}]_{\text{equilibrium}}$, the observed rate constant is given by eq 3, in accordance with reaction 2:

$$k_{\text{obs}} = k_{\text{d}} + k_{\text{f}}[\text{M}] \quad (3)$$

The observed rate constant was measured as a function of barium ion concentration, and these data may be used to estimate the rate constants for azacrown– Ba^{2+} complex dissociation, k_{d} , and azacrown– Ba^{2+} complex formation, k_{f} . Although the relative proportions of the isomers of **1** in the sample solution may vary with $[\text{Ba}^{2+}]$, our control studies have established that the kinetic measurements reported here probe specifically the photochemistry of “closed” *cis*-**1**– Ba^{2+} . A linear regression analysis of k_{obs} versus $[\text{Ba}^{2+}]$ (Figure 6; solid line) gives estimated values of $k_{\text{d}} = (1.0 \pm 0.2) \times 10^6 \text{ s}^{-1}$ and $k_{\text{f}} = (4 \pm 1) \times 10^7 \text{ M}^{-1} \text{ s}^{-1}$, which together give an estimated value of $K_{\text{trans}} = (k_{\text{f}}/k_{\text{d}}) = 40 \pm 20 \text{ M}^{-1}$ for the stability constant of Ba^{2+} complexation with the azacrown of *trans*-**1**. This is in reasonable agreement with the value of $70 \pm 15 \text{ M}^{-1}$ obtained previously from steady-state complexation studies.¹⁹ The data may alternatively be fitted according to eq 4:

$$k_{\text{obs}} = k_{\text{d}} + k_{\text{d}}K_{\text{trans}}[\text{M}] \quad (4)$$

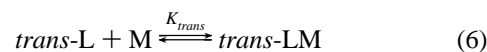
where the value of $K_{\text{trans}} = 70 \text{ M}^{-1}$ from the steady-state studies is fixed. Such an analysis (Figure 6; dotted line) gives estimated values of $k_{\text{d}} = (0.7 \pm 0.2) \times 10^6 \text{ s}^{-1}$ and $k_{\text{f}} = (5 \pm 1) \times 10^7 \text{ M}^{-1} \text{ s}^{-1}$, similar to the values estimated above. In addition to yielding estimates for these rate constants, the ratio of their values indicates that the stability constant for formation of the complex observed on the nanosecond time scale is similar, within error, to that obtained for steady-state complexation of Ba^{2+} to the azacrown of *trans*-**1**. Along with the similarities in the difference spectra, this suggests that the structures of these complexes also are similar.

The dependence of the observed rate constant on temperature can be used to obtain the dependence of k_{d} on temperature, according eq 5:

$$k_{\text{d}}(T) = k_{\text{obs}}(T)/\{1 + K_{\text{trans}}(T)[\text{M}]\} \quad (5)$$

The observed rate constant was obtained as a function of temperature by nanosecond time-resolved studies, but the stability constant for complexation as a function of temperature, $K_{\text{trans}}(T)$, is also required to calculate $k_{\text{d}}(T)$. Assuming that the complex observed in the time-resolved studies is *trans*-**1** with Ba^{2+} complexed by the azacrown, as discussed above, then $K_{\text{trans}}(T)$ can be obtained from an analysis of the steady-state data for Ba^{2+} complexation to the azacrown of *trans*-**1** as a function of temperature.

The steady-state, temperature-dependent spectra of *trans*-**1** obtained in the absence of Ba^{2+} show the changes in the spectrum of *trans*-**1** in the noncomplexed form (Figure 4a), those in the presence of Ba^{2+} at high concentration show the changes in the spectrum of *trans*-**1** with Ba^{2+} complexed with the azacrown (>98% of mixture) (Figure 4c), and those in the presence of Ba^{2+} at an intermediate concentration show the changes in the spectrum arising from an equilibrium mixture of these species (Figure 4b). If the complexation reaction is described by a simple equilibrium 6, as indicated by earlier studies,^{19,22} then the stability constant at a particular temperature can be obtained from eq 7, where A_{f} and A_{c} are the absorbances of **1** in free and azacrown– Ba^{2+} complexed forms, respectively, A is the absorbance of **1** in the presence of barium at concentration $[\text{M}]$, and the absorbances are measured at the same wavelength:



$$K_{\text{trans}} = \{(A_{\text{f}} - A)/(A - A_{\text{c}})\}/[\text{M}] \quad (7)$$

Thus the data in Figure 4 may be used at selected wavelengths to estimate K_{trans} at several temperatures. $K_{\text{trans}}(T)$ was calculated here from data at 520 and 434 nm, where the largest absorbance changes were observed, and the values obtained agree, within the error of these studies, with that of $K_{\text{trans}} = 70 \pm 15 \text{ M}^{-1}$ at ambient temperature.^{19,22} The temperature dependence of the stability constant for complexation of Ba^{2+} to the azacrown of *trans*-**1** can be used to estimate the enthalpy and entropy changes according to eq 8:²⁴

$$\ln K_{\text{trans}} = -\Delta H/RT + \Delta S/R \quad (8)$$

and a linear regression analysis of the data (Figure 7a) gave values of $\Delta H = -11.3 \pm 1.0 \text{ kJ mol}^{-1}$ and $\Delta S = -1 \pm 4 \text{ J K}^{-1} \text{ mol}^{-1}$ from data taken at 434 nm; similar values of $-9.4 \pm 0.5 \text{ kJ mol}^{-1}$ and $+7 \pm 2 \text{ J K}^{-1} \text{ mol}^{-1}$, respectively, were obtained from data at 520 nm. These values are consistent with those reported for many different crown ethers.^{4,25}

With these values of $K_{\text{trans}}(T)$ obtained from the steady-state studies and the values of $k_{\text{obs}}(T)$ obtained from the time-resolved studies, k_{d} may be calculated as a function of temperature according to eq 5. The calculated values of k_{d} may then be used in an Arrhenius plot, according to eq 9:

$$\ln k = \ln A - (E_{\text{a}}/RT) \quad (9)$$

The value estimated from this plot (Figure 7b) for the activation energy for dissociation is $E_{\text{d}} = 38 \pm 15 \text{ kJ mol}^{-1}$. Similarly, the dependence of k_{f} on temperature was calculated using $k_{\text{f}}(T) = k_{\text{d}}(T) K_{\text{trans}}(T)$, and an Arrhenius plot (Figure 7c) gave the activation energy for complex formation as $E_{\text{f}} = 29 \pm 15 \text{ kJ mol}^{-1}$. Although there is a relatively large uncertainty in the actual values, it is clear that both k_{f} and k_{d} increase with increasing temperature, whereas K_{trans} decreases.

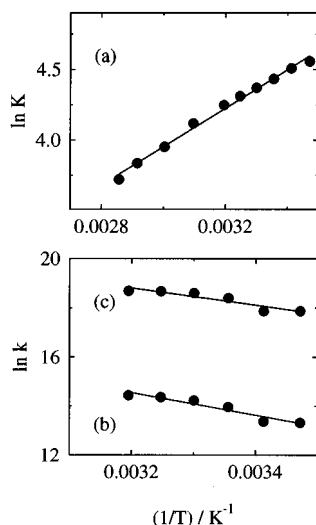


Figure 7. Arrhenius plots of the temperature dependence of (a) K_{trans} , fitted to eq 8, and (b) k_d and (c) k_f fitted to eq 9.

TABLE 1: Rate Constants, Stability Constants, and Activation Energies for Complexes of **1^a and 18-Crown-6 Ether^b with Ba^{2+} in Acetonitrile Solution**

ionophore	k_d/s^{-1}	$k_f/M^{-1} s^{-1}$	K_{trans}/M^{-1}	$E_d/kJ mol^{-1}$
1	1.0×10^6	4×10^7	70	38
18-C-6	1.1×10^3	$>1 \times 10^8$	$>10^5$	32.6

^a k_d , k_f , and E_d from the time-resolved studies reported here; K_{trans} from steady-state studies reported in ref 19. ^b From ref 26.

The values obtained here for the complexation of Ba^{2+} with the azacrown of *trans*-**1** in acetonitrile may be compared with those reported for the complexation of Ba^{2+} with 18-crown-6 ether in acetonitrile, as given in Table 1.²⁶ The activation energies for barium dissociation from the azacrown of *trans*-**1** and from 18-crown-6, of $38 \pm 15 kJ mol^{-1}$ and $32.6 kJ mol^{-1}$, respectively, are similar. In contrast, the rate constants of $k_f = (4 \pm 1) \times 10^7 M^{-1} s^{-1}$ and $k_d = (1.0 \pm 0.2) \times 10^6 s^{-1}$ for **1** are quite different from those of $k_f > 1 \times 10^8 M^{-1} s^{-1}$ and $k_d = 1.1 \times 10^3 s^{-1}$ for 18-crown-6. The stability constant for barium complexation with the azacrown of *trans*-**1**, $K_{trans} = 70 \pm 15 M^{-1}$, is much lower than that of $K > 10^5 M^{-1}$ for barium complexation with 18-crown-6, reflecting the different ratios of the rate constants. The rate constant for Ba^{2+} complex formation is smaller, and that for dissociation is much larger, for the azacrown of *trans*-**1** than for 18-crown-6. This indicates that both formation and dissociation processes contribute to the lower stability constant for Ba^{2+} complexation that is observed for *trans*-**1** in comparison with 18-crown-6. The difference between these values may be attributed to the presence of a partial positive charge at the azacrown nitrogen in *trans*-**1**, which results from an intramolecular charge-transfer resonance form that disfavors cation complexation and which does not contribute to the charge distribution within the simple 18-crown-6 structure.^{20,22}

In summary, the overall mechanism for the photoprocess studied here consists of several steps, as illustrated schematically in Figure 5. Continuous visible irradiation of *trans*-**1** in the presence of $Ba(ClO_4)_2$ at ca. $10^{-4} M$ results in the formation of a photostationary-state mixture in which “closed” *cis*-**1**- Ba^{2+} is dominant. A UV pulse then photolyzes this complex preferentially and results in ultrafast *cis*-*trans* isomerization and the formation initially of a *trans*-**1** complex in which Ba^{2+} is located within the azacrown ether cavity. The barium is then released from the azacrown cavity in ca. 700 ns. The thermal equilibrium, in which the Ba^{2+}/SO_3^- associated *trans*-isomer

is dominant, is re-established. Finally, the photostationary state, in which the “closed” *cis*-**1**- Ba^{2+} form is dominant, is re-established in ca. 30 s by the continuous irradiation beam.

The transient spectra and kinetics indicate that the barium cation remains bound initially to the azacrown on *cis*-*trans* photoisomerization, rather than remaining associated initially with the sulfonate group. Although the stability constant for Ba^{2+}/SO_3^- association is ca. 10^3 times higher than that for Ba^{2+} -azacrown complexation,¹⁹ it is not the relative values of these stability constants that determines the relative yields of these initial photoproducts on isomerization of “closed” *cis*-**1**- Ba^{2+} . Rather, this branching ratio will be determined by the ratio of the rate constants for barium dissociation from the azacrown and from the sulfonate group in the excited state of the “closed” *cis*-**1**- Ba^{2+} complex which undergoes *cis*-*trans* isomerization. These rate constants are not known, but an estimate of their magnitudes for the ground state of *trans*-**1** suggests that they may be similar despite the large difference in K .

Two processes are required to re-establish the thermal equilibrium after the generation of the initial form of *trans*-**1** produced on UV photolysis: the release of Ba^{2+} from the azacrown, and the association of Ba^{2+} with the free sulfonate group. The data indicate that the cation is released in ca. $1 \mu s$, with $k_d \approx 1 \times 10^6 s^{-1}$. The rate constant for Ba^{2+}/SO_3^- association from bulk solution may be expected to approach the diffusion-controlled limit, and thus the time scale for association at these Ba^{2+} concentrations may be estimated to be $1/k_f \geq 1 \mu s$, from $k_f = k_{diffusion}[Ba^{2+}] \approx \leq 10^{10} \times 10^{-4}$. Thus, the thermal equilibrium for *trans*-**1** may be expected to re-establish on the microsecond time scale.

It is possible that intramolecular interaction between the free sulfonate and the decomplexing cation may occur to facilitate Ba^{2+}/SO_3^- association, but several factors suggest that this is not significant. First, a “closed” form of the *trans*-isomer has not been observed, and this absence has been attributed to steric factors preventing the approach of the sulfonate to the azacrown. Second, the stability constant estimated for Ba^{2+} complexation with the azacrown of *trans*-**1** from the time-resolved studies is within the error of that obtained from steady-state studies, in which the sulfonate cannot provide such an interaction because it is already in the Ba^{2+}/SO_3^- associated form.

Conclusions

Nanosecond time-resolved UV-visible absorption spectroscopy has enabled the kinetics and mechanism of the light-triggered release of Ba^{2+} from **1** to be studied directly. The detailed mechanism that we have been able to derive for the reactions observed on photolysis of “closed” *cis*-**1**- Ba^{2+} indicates that the structure of the initial intermediate produced on photolysis, in which the Ba^{2+} cation remains complexed with the azacrown of *trans*-**1**, is not accessed by thermal chemistry at the barium ion concentrations used in this study and that it is the thermal release of the cation from this initial photoproduct that determines the overall rate of release. Thus, both photochemical and thermal mechanisms are involved in controlling ion release from this molecule. The elucidation of such subtleties in the mechanism, obtained here by direct spectroscopic observation and by determining the kinetics and thermodynamics that control the route of the reaction, demonstrates the value of time-resolved techniques for the study of this class of reactions. This study has demonstrated that sustained, photocontrolled ion release from an azacrown ether dye can be achieved within $1 \mu s$ of photolysis. These results may be used to inform strategies for improved molecular design, and the

strategy developed for this study may be applicable for quantitative studies of other cations and other dyes, which may be expected to exhibit different photocontrolled ion-complexing properties.

Acknowledgment. We thank Dr. D. Dukic for technical assistance with the nanosecond laser apparatus, and Prof. M. V. Alfimov and Dr. O. A. Fedorova for providing the sample of **1**. We acknowledge the support of DuPont and EPSRC, the latter through research grant and Advanced Fellowship (J.N.M.) awards.

References and Notes

- (1) Lehn, J.-M. *Supramolecular Chemistry. Concepts and Perspectives*; VCH: Weinheim, 1995.
- (2) Cooper, S. R., Ed. *Crown Compounds: Toward Future Applications*; VCH Publishers, Inc.: New York, 1992.
- (3) Shinkai, S. In *Cation Binding by Macrocycles. Complexation of Cationic Species by Crown Ethers*; Inoue, Y., Gokel, G. W., Eds.; Marcel Dekker, Inc.: New York and Basel, 1990; Chapter 9, pp 397–428.
- (4) Izatt, R. M.; Pawlak, K.; Bradshaw, J. S.; Bruening, R. L. *Chem. Rev.* **1995**, *95*, 2529.
- (5) Eyring, E. M.; Petrucci, S. In *Cation Binding by Macrocycles: Complexation of Cationic Species by Crown Ethers*; Inoue, Y., Gokel, G. W., Eds.; Marcel Dekker, Inc.: New York and Basel, 1990; Chapter 4, pp 179–202.
- (6) Liesegang, G. W.; Eyring, E. M. In *Synthetic Multidentate Macrocyclic Compounds*; Izatt, R. M., Christensen, J. J., Eds.; Academic Press: New York, 1978, pp 245–287.
- (7) de Silva, A. P.; McCoy, C. P. *Chem. Ind.* **1994**, 992.
- (8) Kimura, K. *Coord. Chem. Rev.* **1996**, *148*, 41.
- (9) Kimura, K.; Yamashita, T.; Yokoyama, M. *J. Chem. Soc., Perkin Trans. 2* **1992**, 613.
- (10) Kimura, K.; Yamashita, T.; Yokoyama, M. *Chem. Lett.* **1991**, 965.
- (11) Delmond, S.; Letard, J. F.; Lapouyade, R.; Mathevet, R.; Jonusauskas, G.; Rulliere, C. *New J. Chem.* **1996**, *20*, 861.
- (12) Jonusauskas, G.; Lapouyade, R.; Delmond, S.; Letard, J. F.; Rulliere, C. *J. Chim. Phys.* **1996**, *93*, 1670.
- (13) Martin, M. M.; Plaza, P.; Meyer, Y. H.; Badaoui, F.; Bourson, J.; Lefevre, J.-P.; Valeur, B. *J. Phys. Chem.* **1996**, *100*, 6879.
- (14) Valeur, B.; Bardez, E. *Chem. Brit.* **1995**, *31*, 216.
- (15) Dumon, P.; Jonusauskas, G.; Dupuy, F.; Pee, P.; Rulliere, C.; Letard, J.-F.; Lapouyade, R. *J. Phys. Chem.* **1994**, *98*, 10391.
- (16) Martin, M. M.; Plaza, P.; Dai Hung, N.; Meyer, Y. H.; Bourson, J.; Valeur, B. *Chem. Phys. Lett.* **1993**, *202*, 425.
- (17) Grell, E.; Warmuth, R. *Pure Appl. Chem.* **1993**, 373.
- (18) Alfimov, M. V.; Gromov, S. P.; Lednev, I. K. *Chem. Phys. Lett.* **1991**, *185*, 455.
- (19) Lednev, I. K.; Hester, R. E.; Moore, J. N. *J. Am. Chem. Soc.* **1997**, *119*, 3456.
- (20) Lednev, I. K.; Ye, T.-Q.; Hester, R. E.; Moore, J. N. *J. Phys. Chem. A* **1997**, *101*, 4966.
- (21) Lednev, I. K.; Fyedorova, O. A.; Gromov, S. P.; Alfimov, M. V.; Moore, J. N.; Hester, R. E. *Spectrochim. Acta* **1993**, *49a*, 1055.
- (22) Lednev, I. K.; Hester, R. E.; Moore, J. N. *J. Chem. Soc., Faraday Trans.* **1997**, *93*, 1551.
- (23) Gromov, S. P.; Ushakov, E. N.; Fedorova, O. A.; Soldatenkova, V. A.; Alfimov, M. V. *Izv. Akad. Nauk, Ser. Khim.*, submitted.
- (24) Inou, Y.; Liu, Y.; Hakushi, T. In *Cation Binding by Macrocycles. Complexation of Cationic Species by Crown Ethers*; Inoue, Y., Gokel, G. W., Eds.; Marcel Dekker, Inc.: New York and Basel, 1990; pp 1–110.
- (25) Izatt, R. M.; Pawlak, K.; Bradshaw, J. S.; Bruening, R. L. *Chem. Rev.* **1991**, *91*, 1721.
- (26) Kazem, M.; Shamsipur, M. *J. Phys. Chem.* **1991**, *95*, 9601.